International Journal of the Korean Society of Precision Engineering, Vol. 4, No. 3, May 2003.

Effects of the Grinding Conditions on the Shape of Center Ground Parts

Kang Kim[1, #]

[1] School of Mechanical and Automotive Engineering, Kookmin University, Seoul, South Korea

ABSTRACT

The form accuracy of parts has become an important parameter. Therefore, not only dimensional tolerance but also geometric tolerances are used in the design stage to satisfy the required quality and functions of parts. But the information on the machining conditions, which can satisfy the assigned geometric tolerance in design, is insufficient. The objectives of this research are to study the effects of the grinding parameters such as traverse speed, work speed, depth of cut, and dwell time on the after-ground workpiece shape, and to find out the major parameters among them. The results are as follows; The effects of work speed and depth of cut on the workpiece shape are negligible compared with the effect of traverse speed. These is an optimal dwell time depending on the traverse speed. The optimal dwell time is decreasing as the traverse speed is increasing.

Key Words : Cylindrical grinding, Machining elasticity parameter, Straightness, Traverse speed, Dwell time

1. Introduction

Most of precision mechanical parts have cylindrical shapes, and are manufactured by grinding processes after turning processes normally. Cylindricity, roundness, and straightness are available for defining the geometrical tolerance of the parts. It has been well known that the geometrical tolerances are affected by manufacturing process and conditions (e.g. types of machine, tool, workpiece, and cutting conditions etc.). The geometrical tolerances of cylindrically ground parts were studied on the effects of workpiece supporting centers and machine tool conditions on them mainly. The followings are the representative research works on this area.

Kato and Nakano[1,2] presented the research result that showed the effects of the shape, size, and misalignment of both centers on workpiece. Willmore[3] studied on the influences of the infeed rate on the roundness, straightness, and surface roughness. Rao and Mu[4] proposed the way that can reduce the out of roundness error, which caused by the run-out error between workpiece and grinding wheel axes. Kyusojin[5,6] compared a ball center with a cone center, and also revealed the characteristics of the ball center on the geometrical accuracy of workpiece ground by cylindrical grinding.

So far, there have not been many research works on the effects of grinding conditions, which can be easily controlled by an operator. Thus, the effects of grinding conditions (the traverse speed, depth of cut, work speed, and dwell time) on the shape of cylindrically ground workpieces are carried out in this study through experiment and simulation.

2. Cylindrical Grinding

Fig. 1 shows the relationship between the grinding force acting on the workpiece and the material removal rate. As shown in this figure, there is no essential material removal, even if there are real contacts between the workpiece and grinding wheel. The true material removal occurs when the normal grinding force reaches a

Corresponding Author :
Email : kangkim@kookmin.ac.kr
Tel. +82-2-910-4676

certain limit value. Above the value, the force is proportional to the apparent depth of cut.[7,8] So, the true depth of cut is always smaller than the apparent depth of cut. This phenomenon can be explained by introducing the machining elasticity parameter, κ. κ is a real number which is less than 1, and defines the elastic deformation phenomena in the machine and workpiece system. This is not revealed clearly, but known to vary depending on the grinding condition.

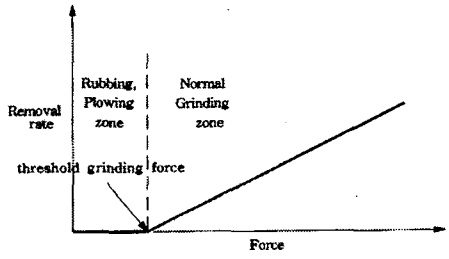

Fig. 1 Effect of normal grinding force on the material removal rate

During the cylindrical grinding process a grinding wheel rotates, and a workpiece not only rotates but also moves reciprocally in the axial direction. Fig. 2 shows the axial traverse distance during one revolution of workpiece and the machining elasticity phenomena. The traverse distance during one revolution of workpiece S_t is proportional to the workpiece traverse speed V_t, and is inversely proportional to the workpiece surface speed V_w. So, S_t can be expressed by

$$S_t = \frac{\pi d_w V_t}{V_w} \tag{1}$$

where d_w is the workpiece diameter.

As shown in Fig. 2, the apparent depth of cut for each grit on the same contact line of the grinding wheel is not equal. The movement of the workpiece makes new grits contact the grinding wheel surface. So, material on the workpiece surface is removed gradually.

If there is an imaginary grinding disk whose width is equal to S_t, the grinding wheel can be supposed as multi-layer lamination of the imaginary grinding disks. Then, it is possible to treat the real continuous cylindrical traverse grinding as a discrete step axial traverse cylindrical grinding using laminated imaginary grinding disks. In this step traverse grinding, the amount of one step traverse is the same as the depth of the imaginary grinding disk. Each disk moves S_t along the traverse direction in every revolution of the workpiece. And, the traverse direction is reversed at the both ends of the ground region in the workpiece. So, the number of contact chances of each grinding disk around its both ends is relatively smaller than that around its middle. Therefore, the amount of material removed around the both ends is less than that around the middle. It causes the difference in diameters along the workpiece axis. In order to reduce this difference, it is recommended that the grinding wheel is staying for a short time at the both ends just before the traverse direction changes. This operation is called dwell. This imaginary grinding wheel and operation makes it easier to develop a model that can be used to analyze the local elastic deformation in the grinding wheel and workpiece system.

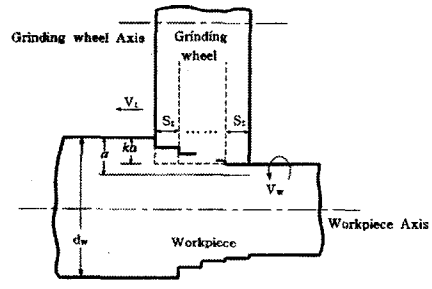

Fig. 2 External cylindrical traverse grinding showing exaggerated wheel surface due to machining elasticity

In most cases, the surface speed of the grinding wheel is constant. The shorter the axial traverse distance during one revolution of workpiece S_t makes the more contact chances between the grinding wheel and workpiece. Generally, the traverse speed of the workpiece is equivalent to 2/3~3/4 of the width of grinding wheel for one revolution of workpiece in rough grinding. For fine grinding, 1/4~1/2 of the width is recommended.[9]

3. Experiments

The cylindrical grinding machine used in experiments was GAU25-50L manufactured by Miyamoto Co. The specimen was made from a general purpose carbon steel (SM45C), and heat-treated by high frequency induction

hardening. Before heat treatment, it was prepared as a cylindrical bar (diameter: 30mm, length: 200mm) with center holes at both ends (diameter: 3mm, depth: 5mm). Because the deformation caused by heat treatment, the center holes were re-drilled using a ϕ 5mm center drill after the heat treatment. Specimen was held between both centers at headstock and tailstock, and driven using a drive plate and a dog. Because of the interference between wheel and centers, 40mm regions from both ends were excluded from the ground region. So, the traverse distance was 120mm. The radial depth of cut was applied during dwell at the tailstock side. Spark-out operation was done three times.

Details on the experimental conditions are shown in Tables 1 and 2. In experiment 1, the surface speed of specimen, the traverse speed, and the radial depth of cut were varied to investigate the characteristics of geometrical shape according to grinding condition. The goal of experiment 2 is to investigate the effects of the traverse speed and dwell time on the geometrical shape.

Table 1 Experiment conditions (Experiment 1)

Fixed	
grinding wheel type	WA60L7V30
grinding wheel speed (rpm)	1740
dwell time (sec)	2
No. of spark-out	3
Variable	
traverse speed (m/min)	0.130, 0.714, 1.630
workpiece surface speed (m/min)	6.16, 14.6, 24.5, 33.46
radial depth of cut (mm/path× No. of path)	0.0125×8, 0.0250×4, 0.0375×3, 0.0500×2

Table 2 Experiment conditions (Experiment 2)

Fixed	
grinding wheel type	WA60L7V30
grinding wheel speed (rpm)	1740
workpiece surface speed (m/min)	14.6
No. of spark-out	3
radial depth of cut (mm)	0.0125
Variable	
traverse speed (m/min)	0.130, 0.714, 1.630
dwell time (sec)	2, 4, 6

Cylindricity, roundness, and straightness were measured using a Talyrond 250 system. For cylindricity and roundness measurements, 11 layers along the axis were selected. The distance between two adjacent layers was 10mm. To measure the straightness, a stylus was moved 100mm on the ground surface parallel to the axis of the specimen with constant speed.

4. Simulation Model

Because before-grinding shape of the specimen is axi-symmetric, it is also assumed that after-ground shape is axi-symmetric. Therefore, it is possible to get 3-D surface information through a straightness simulation on the contour of the cross-section including the specimen axis. If the interference phenomena in cylindrical grinding is ignored, every point on the cylindrical surface of the specimen meets the grinding wheel only once in every 360° rotation of the specimen. Furthermore, every point which contacts the grinding wheel at the same time has different axial displacement and true depth of cut when the apparent depth of cut a is constant. Thus, the traverse cylindrical grinding process can be modeled as an imaginary grinding process in which a pseudo grinding wheel (being laminated n imaginary grinding disk with width S_t) removes the surface of a pseudo workpiece (being laminated m imaginary workpiece disk with width S_t) under an intermittent traverse S_t in every 360° rotation of the workpiece. In general, the workpiece length is larger than the grinding wheel width. This means that m is always greater than n.

If the number of workpiece rotations per minute is N_w and the first grinding disk engages the lth workpiece disk, the length of the instant time t is

$$t = (1 / N_w) \times l \qquad (0 \le l \le m\text{-}n) \tag{2}$$

If the ith grinding disk G_i engages the jth workpiece disk W_j at the same time, j is given by

$$j = n + l - (i - 1) \tag{3}$$

Therefore, the true depth of cut of W_j by G_i at this instant $d_{j,l}$ is

$$d_{j,l} = a_{j,l} - a_{j,l+1} = \kappa (a_{j,l}) \tag{4}$$

where $a_{j,l}$ is the apparent depth of cut, and $a_{j,l+1}$ is the depth of cut being not removed just after this instant

because of the machining elasticity phenomena. κ is defined as a ratio between the true depth of cut and apparent depth of cut. Thus,

$$\begin{aligned} a_{j,l+1} &= (1-\kappa)(a_{j,l}) \\ &= (1-\kappa)[(1-\kappa)(a_{j,l-1})] \\ &\vdots \\ &\vdots \\ &= (1-\kappa)^i (a_{j,l-(i-1)}) \end{aligned} \tag{5}$$

where $a_{j,l-(i-1)}$ is the radial depth of cut applied at the dwell time. And the dwell time is converted as an equivalent number of workpiece rotations. It is assumed that there is no change in both of grinding disk and workpiece disk during the dwell operation.

Thus, if the value of the machining elasticity parameter κ is known, it is possible to estimate the during-grinding and after-ground shapes easily using this simulation model.

5. Machining Elasticity Parameter

There are local elastic deformations in the grinding wheel and workpiece system. As shown in Fig. 3, the true depth of cut is less than the apparent depth of cut a, when the grinding wheel is moved from A to B. If the true depth of cut is equivalent to the apparent depth of cut multiplied by an arbitrary number, this number is the machining elasticity parameter κ.

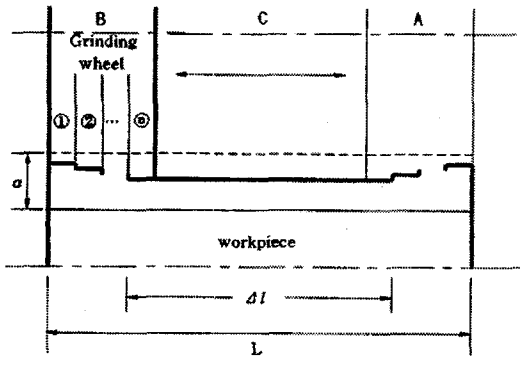

Fig. 3 Schematic illustration of grinding wheel deflection

To find the value of κ experimentally, it is assumed that κ is constant in every axial traverse. If the grinding wheel traverses from A to B just after the radial depth of cut a_i applied, the diametral difference between before and after the traverse in the middle of the workpiece (Δl) can be measured. The half of this diametral difference is the true depth of cut. So, if the width of grinding wheel is equal to the total width of the n-layered grinding disks approximately, the un-removed depth of cut is

$$a_{i+1} = (1-\kappa)^n a_i \tag{6}$$

Thus κ is expressed as a function of measurable variables. The following shows this function.

$$\kappa = 1 - (a_{i+1} / a_i)^{(1/n)} \tag{7}$$

Table 3 shows the machining elasticity parameter values calculated by the equation (7) using the experimental data. In the experiment, the apparent depth of cut was 0.050mm, and applied only once at the end of the tailstock side. Through this experiment, it was revealed that the machining elasticity parameter value decreases when the number of axial traverses increases.

Table 3 Machining elasticity parameter (experimental result)

traverse speed (V_t)(m/min)	path	diameter (mm)		κ
		before	after	
0.130	tail → head	29.675	29.582	0.0574
	head → tail	29.582	29.580	0.028
	tail → head	29.580	29.580	0.01
	head → tail	29.580	29.580	0.01
0.714	tail → head	29.746	29.664	0.193
	head → tail	29.664	29.653	0.114
	tail → head	29.653	29.649	0.108
	head → tail	29.649	29.648	0.05
1.630	tail → head	29.729	29.668	0.2097
	head → tail	29.668	29.652	0.1236
	tail → head	29.652	29.647	0.0594
	head → tail	29.647	29.642	0.0781

6. Results and Discussion

6.1 Grinding condition

The measured results in experiment 1 are shown in Table 4. The roundness values in this table are the average values of the roundness measured in each layer

for the same specimen.

Table 4 Grinding results in each condition

test No.	workpiece surface speed (m/min)	traverse speed (m/min)	depth of cut (μm)	straight-ness (μm)	cylin-dricity (μm)	straight-ness (μm)
1	6.16	0.130	125	1.58	4.30	2.50
2			250	1.48	3.90	2.35
3			375	1.20	3.40	2.45
4			500	1.01	3.75	2.60
5		0.714	125	1.21	5.15	1.75
6			250	2.94	9.00	2.10
7			375	1.66	4.15	1.95
8			500	1.30	2.75	2.10
9		1.630	125	1.44	2.25	1.60
10			250	1.83	3.25	1.85
11			375	1.92	3.95	2.65
12			500	1.87	4.20	3.40
13	14.5	0.130	125	0.65	5.10	2.80
14			250	0.65	3.85	2.45
15			375	0.63	3.60	2.60
16			500	0.62	4.00	2.50
17		0.714	125	1.58	4.25	2.00
18			250	1.96	5.60	1.75
19			375	1.38	3.70	1.80
20			500	1.15	3.05	1.90
21		1.630	125	1.47	2.95	1.00
22			250	1.88	4.55	1.15
23			375	1.70	4.00	1.55
24			500	2.36	5.25	2.20
25	24.5	0.130	125	0.74	3.20	2.25
26			250	0.74	3.20	2.00
27			375	1.43	4.00	2.00
28			500	1.30	3.90	2.45
29		0.714	125	1.00	3.90	1.30
30			250	1.12	3.90	1.55
31			375	1.13	6.05	1.55
32			500	1.48	6.80	1.95
33		1.630	125	1.50	6.00	1.40
34			250	1.14	5.50	2.35
35			375	1.43	7.60	1.80
36			500	1.55	5.20	2.30
37	33.5	0.130	125	0.57	4.10	2.25
38			250	0.61	2.60	2.00
39			375	0.80	2.85	1.95
40			500	0.81	3.55	2.05
41		0.714	125	0.93	3.70	1.55
42			250	1.37	5.50	1.75
43			375	0.84	3.45	1.55
44			500	1.21	3.90	2.05
45		1.630	125	1.52	5.75	3.05
46			250	1.36	8.10	3.05
47			375	1.60	9.05	3.55
48			500	2.70	12.50	4.70

This table shows that the cylindricity implying 3-D geometrical accuracy has relatively stronger relation with the straightness than the roundness. As mentioned before, the workpiece rotates and becomes an axi-symmetrically shaped part in traverse cylindrical grinding. So, it is also possible to eliminate a taper error, because the shape of the specimen was bilaterally symmetric. Thus, characteristics of the after-ground shape can be analyzed from the viewpoint of straightness mainly.

Among workpiece surface speed, traverse speed, and apparent depth of cut, the traverse speed is the most important factor that affects the after-ground shape. Because the surface speed of the grinding wheel is much faster than that of the workpiece, variation of workpiece surface speed causes only a little change in the grinding speed, which is defined as a relative surface speed between the grinding wheel and workpiece at the contact point. For repetitive traverse motion, the traverse speed and direction must be changed around the both ends of the grinding region before and after the dwell. So, it is found that there are bigger changes in straightness than any other ground surfaces of the specimen.

6.2 Traverse speed and dwell time

Figs. 4 and 5 show the effects of the traverse speed and dwell time on the straightness of the after-ground workpiece. As shown in Fig. 3, the ground surface is divided into three regions for the convenience of understanding. Regions A, B, and C correspond to the dwell zone near the tailstock side, the dwell zone near the headstock side, and the middle of the ground surface, respectively. The width of the grinding wheel was 38mm. The measurement range was 100mm that is equivalent to the length of the grinding zone excluding 10mm at both ends of the grinding zone. Thus, lengths of A, B, and C are 28mm, 28mm, and 44mm, respectively.

From the experiment results in Fig. 4, it is found that the amount of material removed in region C decreases as the traverse speed increases. It is also shown that the amount of material removed in regions A and B increases as the dwell time increases. If the dwell time is relatively too short in comparison to the traverse speed, the material removal rate at region A or B is slower than that at region C, because region A or B has a lower frequency in grinding wheel contact than region C. Thus, the straightness profile becomes 'U' shaped in this case.

On the contrary, if the dwell time is relatively too long in comparison to the traverse speed, the straightness profile of the workpiece becomes 'W' shaped.

In order to grind a cylindrical workpiece as straight

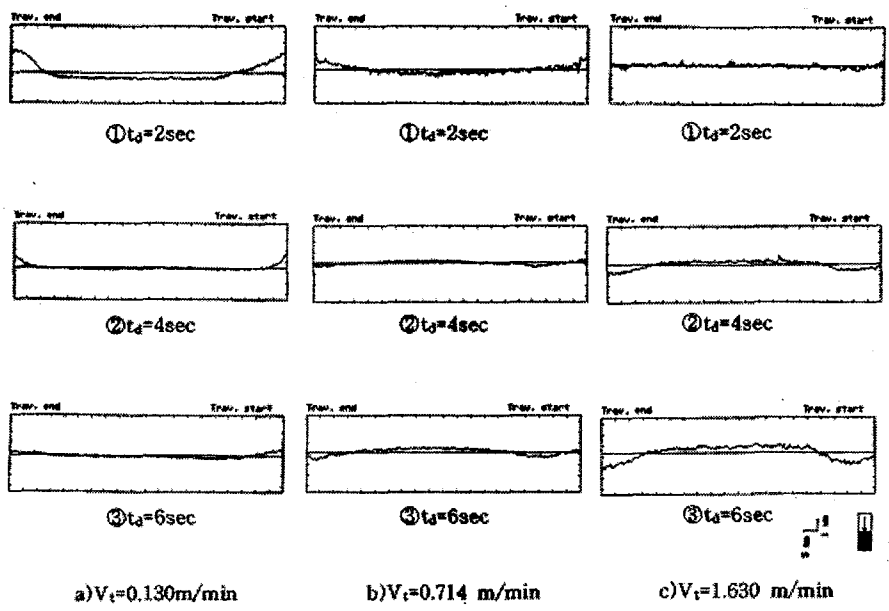

Fig. 4 Straightness profile (experiment) (t_d: dwell time, V_t: traverse speed)

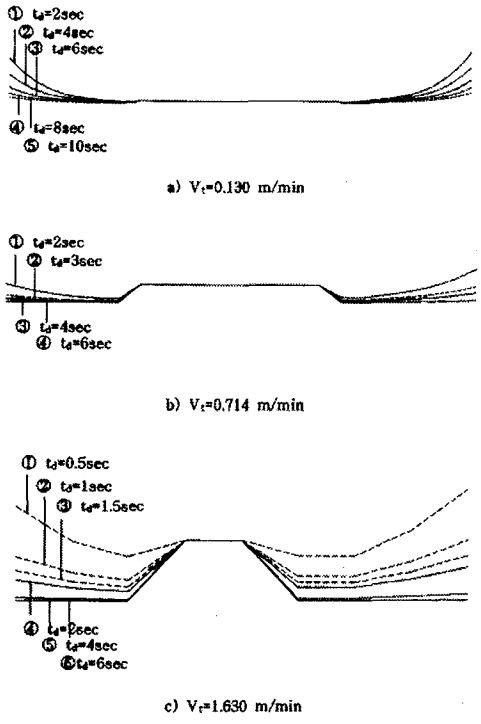

Fig. 5 Straightness profile (simulation)
(t_d: dwell time, V_t: traverse speed)

as possible, the differences in the amount of material removed per unit length along the workpiece axis must be minimized. So, from the viewpoint of straightness, the optimal dwell time has to decrease when the traverse speed increases. The same tendency is found in Fig. 4. When the traverse speed increases from 0.130m/min to 0.714m/min, the dwell times for the best straightness for the two conditions are 6 seconds and 4 seconds, respectively. For even more faster traverse speed condition (1.630m/min), the specimen dwelt for less time (2 seconds) has the best straightness.

The experimental results in Fig. 4 and the simulation results in Fig. 5 show the same qualitative tendencies. But, there are some quantitative differences in the results. Comparison between experiment and simulation results is shown in Table 5. Except for the only one case (traverse speed =1.630m/min, dwell time=2seconds), the differences are less than ± 5%. The followings are the presumed sources of errors in the simulation results in comparison with the experimental results.

- Before-grinding shape is assumed as a perfect cylinder to eliminate the interference phenomena.
- Lengths of the imaginary grinding wheel and

workpiece are always multiples of S_t.

- The time required for applying the depth of cut is ignored.
- The inertia effect caused by high traverse speed is disregarded at both ends

Table 5 Variation of straightness (Experiment, Simulation)

traverse speed(V_t) (m/min)	dwell time(t_d) (sec)	straightness (㎛)		tolerance (%)
		experiment	simulation	
0.13	2	2.70	2.20	1.8
	4	1.65	1.56	0.5
	6	0.95	1.03	-0.9
	8	-	0.73	-
0.714	2	2.15	1.27	4.0
	3	-	0.68	-
	4	0.75	0.70	0.5
	6	1.20	0.73	3.9
1.63	0	-	3.50	-
	1	-	1.58	-
	1.5	-	1.80	-
	2	1.00	1.97	-9.7
	4	1.70	2.28	-3.4
	6	2.15	2.32	-0.8

7. Conclusions

The effects of easily adjustable grinding variables on the after-ground shape in traverse cylindrical grinding were investigated through experiment and simulation. The specimen was axi-symmetric. And it was assumed that there is no movement of the rotational axis of workpiece during grinding. So, it was possible to analyze 3-D shape from the viewpoint of straightness profile. The followings are the results of this study.

- The effects of work speed and depth of cut on the workpiece shape are negligible compared with the effect of traverse speed.
- The optimal dwell time is mainly affected by the traverse speed.
- The optimal dwell time is decreasing as the traverse speed is increasing.

References

1. Kato, H. and Nakano, Y., "Transfer of Roundness Error from Center and Center Hole to Workpiece in Cylindrical Grinding and its Control," Annals of the CIRP, Vol. 34/1, pp. 287~290, 1985.
2. Kato, H. and Nakano, Y., "Effect of Alignment Errors of Centers and Center Holes upon Rotation Accuracy of Workpieces," Bull. Japan Soc. of Precision Engineering, Vol. 20, No. 3, pp. 171~176, Sep. 1986.
3. Willmore, J. I., "Plunge Grinding and the Accuracy of the Workpiece Geometry," Proc. 6th Int'l Mach. Tool Des. and Res. Conf., pp. 543~555, 1965.
4. Rao, S. B. and Mu, S. M., "Compensatory Control of Roundness Error in Cylindrical Chuck Grinding," J. of Engineering for Industry, Vol. 104/23, pp. 23~28, Feb. 1982.
5. Kyusojin, A., Ogawa, K. and Toyama, A., "Comparision of Cone Center and Ball Center for Roundness in Cylindrical Grinding," Precision Engineering, Vol. 8, No. 4, pp. 197~202, Oct. 1986.
6. Kyusojin, A. and Todaka, R., "Development of a Precise Cylindrical Grinding by Using Steel Balls," Bull. Japan Soc. of Precision Engineering, Vol. 22, No. 3, pp. 190~194, Sep. 1988.
7. Suh, N. S., Metal Cutting Theory (Korean), Dongmyung-sa, pp. 363~367, 1991.
8. Dorzda, T. J. and Wick, C., Tool and Manufacturing Engineers Handbook, fourth Edition, volume 1-Machining, SME, pp. 11.109~11.118, 1983.
9. Kim, D. W., Manufacturing Processes (Korean), Chungmoon-gak, pp. 524~525, 1991.